Brain Research 1747 (2020) 147033

Contents lists available at ScienceDirect

Brain Research

journal homepage: www.elsevier.com/locate/brainres

Research report

Detailed morphological analysis of rat hippocampi treated with CSF autoantibodies from patients with anti-NMDAR encephalitis discloses two distinct types of immunostaining patterns

Franziska Wagner[a], Angelika Goertzen[b], Orsolya Kiraly[c], Gregor Laube[d], Jakob Kreye[e], Otto W. Witte[a], Harald Prüss[e,*], Rüdiger W. Veh[c,*]

[a] "Hans Berger" Klinik für Neurologie, Universitätsklinik Jena, An der Klinik 1, D-07747 Jena, Germany
[b] AMEOS Klinikum St. Clemens Oberhausen, Wilhelmstrasse 34, D-46145 Oberhausen, Germany
[c] Institut für Zell- und Neurobiologie, Centrum 2, Charité - Universitätsmedizin Berlin, Charitéplatz 1, D-10117 Berlin, Germany
[d] Institut für Vegetative Anatomie, Centrum 2, Charité - Universitätsmedizin Berlin, Charitéplatz 1, D-10117 Berlin, Germany
[e] Department of Neurology and Experimental Neurology, Charité – Universitätsmedizin Berlin, and German Center for Neurodegenerative Diseases (DZNE) Berlin, Charitéplatz 1, D-10117 Berlin, Germany

HIGHLIGHTS

- Autoantibodies from patients with NMDA-R1 encephalitis show two distinct immunoreactivity patterns in rat hippocampus.
- Antibodies from "pattern group 1" display the familiar pattern of NMDA-R1 subunits.
- Antibodies from "pattern group 2" show an inverse pattern leaving cells and dendrites in CA1 and CA3 regions empty.
- Electron microscopy discloses that group 2 in contrast to group 1 autoantibodies target presynaptic NMDA receptors.

ARTICLE INFO

Keywords:
CNS
Rat
Human cerebrospinal fluid (CSF)
Autoimmune disorders
Presynaptic anti-NMDA-R antibodies
Monoclonal antibodies NMDA receptor encephalitis

ABSTRACT

Anti-NMDA receptor encephalitis was first described about thirteen years ago and has become one of the most important differential diagnoses for new-onset psychosis. The disease is mediated by autoantibodies against the subunit 1 of the N-methyl-D-aspartate receptor (NMDA-R1) in patients presenting with variable clinical symptoms. Patients often profit from immunmodulatory therapy, independent of their individual symptoms.

In this study CSF samples as well as monoclonal antibodies derived from patients diagnosed with NMDA-R1 encephalitis were applied to rat hippocampus and visualized by immunocytochemistry. This reveals at least two distinct patterns of immunoreactivity. Antibodies from "pattern group 1" display the familiar pattern of NMDA-R1 distribution in the hippocampus reported in experiments with rabbit anti-NMDA-R1 antibodies. Neurons and primary dendrites in the CA1 and CA3 region show strongly stained cell bodies, in line with the predominant postsynaptic localization of the NMDA receptor in the brain. However, autoantibodies from "pattern group 2" show an inverse pattern, with no staining of the cell bodies and primary dendrites in CA1 and CA3 regions. Electron microscopic experiments disclose that autoantibodies of "pattern group 1 patients" bind to postsynaptic NMDA receptors, while those of "pattern group 2 patients" target presynaptic NMDA receptors. We describe one NMDA-receptor antibody giving staining comparable to rabbit anti-NMDA-R1 antibodies, raised against the C-

Abbreviations: ABC, avidin biotin-peroxidase complex; CA1, cornu ammonis 1 subregion of the hippocampus proper; CA3, cornu ammonis 3 subregion of the hippocampus proper; cDNA, complementary DNA; DAB, di-amino-benzidine; DG, dentate gyrus subregion of the hippocampus proper; CSF, cerebrospinal fluid; GluN1, common substitute for NMDA-R1; GluN2, common substitute for NMDA-R2; GluN3, common substitute for NMDA-R3; HEK293, human embryonic kidney cells; IF, immunnofluorescence; IP, immunnoperoxidase; NGS, normal goat serum; NMDA-R, N-methyl-D-aspartate receptor; NMDA-R1, subunit 1 of the N-methyl-D-aspartate receptor; NMDA-R1-1a, splice variant 1a of the subunit 1 of the N-methyl-D-aspartate receptor; PBS, phosphate buffered saline; PBS-A, phosphate buffered saline containing 2% bovine serum albumine; RT, room temperature; SO, stratum oriens of the hippocampus proper; SR, stratum radiatum of the hippocampus proper

* Corresponding authors.
E-mail addresses: harald.pruess@charite.de (H. Prüss), ruediger.veh@charite.de (R.W. Veh).

https://doi.org/10.1016/j.brainres.2020.147033
Received 15 April 2020; Received in revised form 23 July 2020; Accepted 24 July 2020
Available online 28 July 2020

terminus. In the highly heterogenous disease anti-NMDA-receptor 1 encephalitis we found evidence for at least two different subtypes. It will be very interesting to determine whether there also are two distinct clinical phenotypes.

1. Introduction

Anti-NMDA receptor encephalitis was first described about thirteen years ago (Dalmau et al., 2007) and has become one of the most important differential diagnoses for new-onset psychosis. The disease is mediated by autoantibodies against one of the ionotropic glutamate receptors (Dalmau et al., 2007), the N-methyl-D-aspartate receptor 1 (NMDA-R1). Patients present with variable clinical symptoms, psychiatric symptoms, memory disturbances, seizures, dyskinesias, autonomic instability, or hypoventilation. The final diagnosis usually is based on laboratory medicine, where CSF antibodies are shown to bind to human embryonic kidney cells transfected with the NMDA-R1 (Peery et al., 2012) or to unfixed cryostat or paraformaldehyde-fixed paraffin sections of the rat hippocampus in a NMDA-R1-like mode as visualized by immunofluorescence (Dalmau et al., 2008). Patients often profit from immunomodulatory therapy (Titulaer et al., 2013, Panzer and Lynch 2013).

The NMDA-R exists as multiple subtypes with differing molecular compositions (Paoletti et al., 2013). It is always composed of two types of proteins, GluN1 (NMDA-R1, NR1) and GluN2 or GluN3 (NMDA-R2/3, NR2/3) subunits, which form a tetrameric channel molecule. Early attempts to identify the relevant target of the autoantibodies revealed a small region within the amino terminal domain of the GluN1 subunit (Gleichman et al., 2012) and indicated that autoantibodies of all patients with NMDA encephalitis always recognize this single epitope.

The pathomechanisms of autoimmune disorders, however, are poorly understood. In general it is assumed that dying or dead cells release components into the extracellular space, where these molecules may provoke an immune response. NMDA-Rs are present in many neuronal cell types and in various molecular forms. Consequently, it expected that CSF-derived autoantibodies against any other epitopes of the NMDA-R1 subunit, against other subunits of NMDA-R, or against auxiliary brain proteins could contribute to the pathophysiology of patients diagnosed with anti-NMDA-R encephalitis.

Accordingly, in the present investigation we applied CSF samples and monoclonal antibodies from patients diagnosed with anti-NMDA-R encephalitis to coronal sections across the rat hippocampus and visualized them using immunocytochemistry. The aim was to learn, whether the CSF samples of different patients always produce a staining pattern identical to the standard found in of anti NMDA-R encephalitis (Dalmau et al., 2008). This is to be expected, if all patient CSFs interact with the same target protein.

2. Results

In neuropsychiatry, the autoantibodies in CSF samples of patients with anti-NMDA receptor encephalitis are usually detected by immunofluorescence (IF) in cell-based assays using HEK cells transfected with N-methyl-D-aspartate receptor 1 (NMDA-R1) cDNA. In uncertain cases, the characteristic immunostaining pattern of rat hippocampal sections is adopted for confirmation (Dalmau et al., 2008; van Coevorden-Hameete et al., 2016; de Witte et al., 2007). This, however, may result in false negative results, when the immunocytochemical protocol does not provide sufficient sensitivity, to detect the low levels of immunoglobulins in CSF samples.

2.1. Unequivocal visualization of tissue bound autoantibodies requires powerful staining techniques

Immunoglobulin concentrations in the CSF usually are very low (0.04 mg/ml) as compared to serum (10 mg/ml). Consequently, only low dilutions of the corresponding CSF samples allow successful staining by IF (Fig. 1A, 1B). Immunoperoxidase (IP) techniques such as the ABC procedure (Hsu and Soban, 1982) are sensitive and have been used successfully for the visualization of autoantibodies in the sera of patients with Guillain-Barré syndrome (Görtzen et al., 2004; Rink et al., 2017).

The striking difference in sensitivities between IF- and IP-techniques is most evident by direct comparison. The CSF of a patient with NMDA-R1 autoimmune encephalitis when analyzed with the IF-procedure at a ten-fold dilution produces a section, which largely remains black (Fig. 1A). Production of the characteristic NMDA-R1-staining in the CA1 area of the hippocampus (Fig. 1B) is only evident at a two-fold dilution of the CSF. However, using the IP-technique, hippocampal staining is very strong at a ten-fold dilution, especially in the CA1 area (Fig. 1D). Even Cthe A3 region and dentate gyrus show distinct immunoreactivities (Fig. 1D), which are completely blank with immunofluorescence (not shown). IP-staining at high magnification (area labeled with two asterisks in Fig. 1D) clearly shows the apical dendrites of CA1 pyramidal neurons (Fig. 1F). These dendrites remain faintly visible, even at much higher dilutions (50-fold; Fig. 1E). The control section is completely blank (Fig. 1C). Consequently, the IP-technique was used for subsequent experiments.

2.2. Patients with NMDA-R encephalitis display different CSF-staining patterns in the rat hippocampus

The most important two areas necessary for analysis of the detailed distribution of NMDA-R1-subunits in the hippocampus are the CA1 region (Fig. 2A, 2B) and the upper blade of the dentate gyrus (DG; Fig. 2A, C). The CA1 region contains a prominent layer of pyramidal cell bodies with large dendrites extending downward to the stratum radiatum (SR) together with axons, leaving the hippocampus upward via the stratum oriens (SO) as depicted in Cajal's schemes (Fig. 2A,B; Ramón y Cajal, 1995). In this area the strongest NMDA-R1 immunoreactivity as visualized with two rabbit anti-NMDA-R1 sera is found along the primary dendrites of the CA1 neurons in the SR (Fig. 2D, E; insets). Note that SO staining is only weak. In the DG NMDA-R1 immunoreactivity is largely restricted to the granule cell bodies (Fig. 2D, E; compare with Fig. 2C). Astrocytes remained unstained in all our sections, in spite of the fact that they are known to express functional NMDA receptors (Lalo et al., 2006).

Surprisingly, the different CSF samples from patients with recognized anti-NMDA-R autoimmune encephalitis yielded at least two distinct patterns when applied to rat hippocampal sections. The CSF samples of one patient group (pattern group 1) produce staining patterns (Fig. 2F, H) very similar to those obtained with recognized rabbit anti-NMDA-R1 immunoglobulins (compare Fig. 2D and E with F and H). Comparable to the commercial rabbit antibodies these CSF samples label pyramidal cell bodies and primary dendrites in the CA1 region and granule cell bodies in the DG most prominently. Staining of the SO in CA1 and the lower molecular layer in the upper blade of the DG only is weak (Fig. 2F, H). In striking contrast, the CSF samples of other patients (pattern group 2) stain SO of the CA1 region much stronger (Fig. 2G) or with similar intensity (Fig. 2I) as compared to the SR. In the DG immunoreactivity is most prominent in the lower molecular layer of the DG (Fig. 2G, I), corresponding to the dense parvalbumin-positive basket cell plexus localized there (Paxinos et al., 1999). This pattern is quite different from the recognized anti-NMDA-R1 pattern as described above.

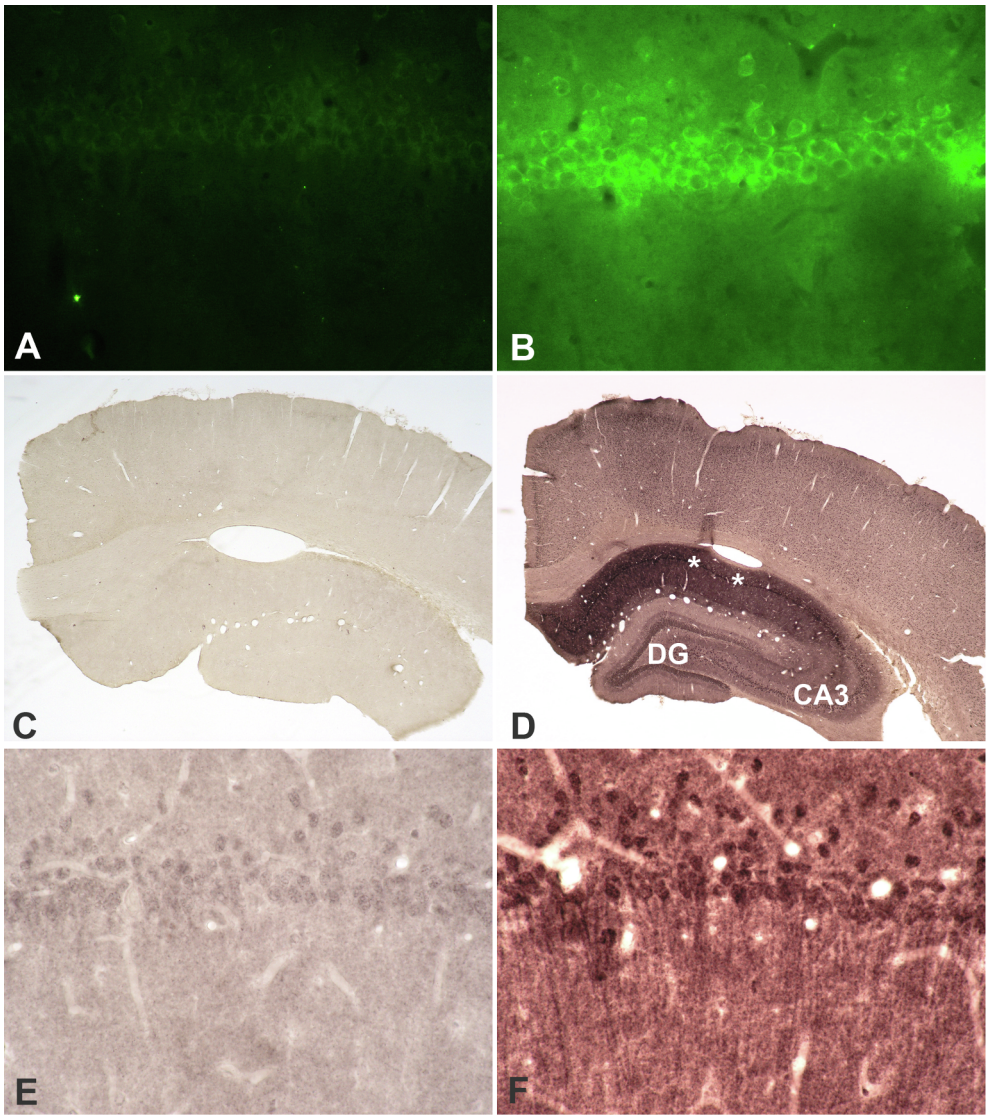

Fig. 1. The ABC immunoperoxidase technique provides a much higher sensitivity as compared to immunofluorescence. CSF of a patient (J-18/40, Table 1) with presumed anti-NMDA receptor encephalitis was applied to coronal sections across the cortex and hippocampus of a rat. Visualization of tissue-bound autoantibodies using immunofluorescence is barely feasible under normal conditions (A; hippocampal CA1 region; CSF J-18/40 at 10-fold dilution). High CSF concentrations are required to obtain successful staining (B; CA1 region; CSF J-18/40 at 2-fold dilution). However, when the ABC immunoperoxidase procedure is used, low CSF concentrations readily result in strong staining of the hippocampal CA1 area (D, white asterisks; CSF J- 18/40 at 10-fold dilution). Even the CA3 and the dentate gyrus display distinct immunoreactivities (D), which are completely absent in immunofluorescence (not shown). At high magnification immunoperoxidase staining of the CA1 area labeled by two asterisks in D clearly shows the apical dendrites of pyramidal neurons (F; CSF J-18/40 at 10-fold dilution). These are faintly visible even at much higher dilution (E; CSF J-18/40 at 50-fold dilution). The control section is completely blank (C). Bar in (F) indicates 600 μm in (C) and (D), and 38 μm in (A), (B), (E), and (F).

2.3. High magnification discloses additional differences between the pattern group 1 and pattern group 2 of patients with anti-NMDAR1-encephalitis

A more detailed analysis of immunostained sections reveals further differences (Fig. 3A, B). Higher magnification of the hippocampal CA1 region in group 1 patients shows that CSF samples react with the cell bodies of the pyramidal neurons and with the main dendrites for a long considerable distance (Fig. 3A, C), corresponding to the distribution of NMDA-R1 subunits visualized with recognized antibodies (compare to Fig. 2D, E; insets). When the CA1 area is treated with CSF samples from pattern group 2 patients, the cell bodies of pyramidal neurons remain unstained (Fig. 3B, D) and even the main dendrites can be recognized as empty elongated spaces between a strongly reactive neuropil (Fig. 3D inset, arrows). A similar difference is apparent when comparing the CA3 area (Fig. 3E, F), where group 2 CSF samples do not stain the stratum lucidum. In the upper blade of the DG cell bodies of granule cells as well as those of interneurons beneath strong staining of the pattern group 1 CSF samples is found (Fig. 3E). In contrast, CSF samples of pattern group 2 patients do not react with granule cell bodies. However, strong immunoreactivity is found in the neuropil of the lower molecular layer, very similar to the pattern obtained with the other two CSF samples from the same group (Fig. 2G and I). Such striking differences are very interesting, when especially considering that all these patients were diagnosed as suffering from anti-NMDA receptor autoimmune encephalitis (see discussion).

2.4. Blocking experiments confirm that CSF samples of pattern group 2 patients do interact with the NR1 subunit of NMDA receptors

The striking differences in the staining patterns between CSF samples or monoclonals of pattern group 1 and pattern group 2 patients suggest that competition experiments would be appropriate. Consequently, two types of blocking experiments were designed (Table 3). In the first set, the monoclonal antibody (003-102) of a pattern group 2 patient was used to stain hippocampal sections (see Table 3, experiment 1a) yielding the characteristic pattern for this group with a strongly stained SO in the CA1 field and empty cell bodies in the CA1 pyramidal cell layer and the DG granule cell layer as expected (Fig. 4B, C, D). The adjacent section (Table 3, experiment 1b) was treated with the rabbit anti-NMDA-R1 antibody prior to the pattern

group 2 CSF and visualized with anti-human secondary antibody. This yielded a relatively intact reaction with the human CSF (Fig. 4E, G; Table 3). This experiment indicates that the pattern group 2 CSF interacts with a NMDA-R1 epitope distinct from the rabbit one.

In the second set of experiments, the rabbit anti-NMDA-R1 receptor antibody was used (Table 3, experiment 2a) to stain hippocampal sections, yielding the characteristic distribution of NMDA-R1 staining in the hippocampus (Fig. 2D, E). However, when the adjacent section was pretreated with the monoclonal antibody of a pattern group 2 patient before the rabbit anti-NMDA-R1 antibody (Table 3, experiment 2b), visualization with the anti-rabbit secondary antibody was completely abolished (Fig. 4E, G; Table 3). This supports the idea that the monoclonal antibody (003-102) of the pattern group 2 patient indeed interacts with the NMDA-R1 subunit at an epitope, which is identical or at least closely located to the one recognized by the rabbit antibody.

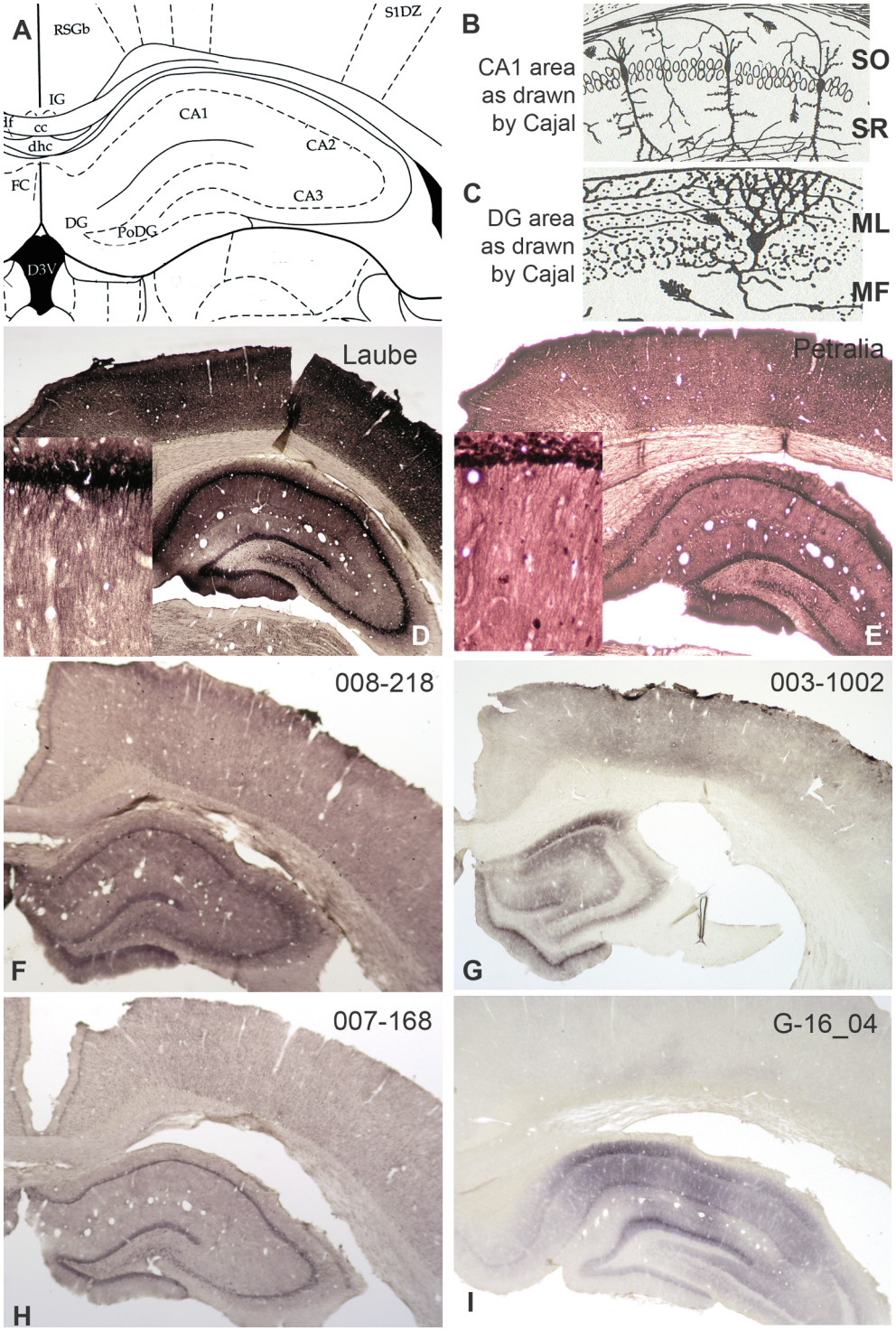

Fig. 2. Patients with NMDA-encephalitis display two different CSF-staining patterns in the rat hippocampus. A more detailed analysis of the distribution pattern of the NMDA-R1 subunit requires a basic knowledge of the hippocampal area. The schematic representation (A) of the hippocampus in the rat (Paxinos and Watson, 1998) displays the major subareas of the hippocampus proper, the CA1-, the CA2-, and the CA3-region and the dentate gyrus (DG). Typical neuronal profiles of CA1 pyramidal neurons (B) and DG granule neurons (C) were drawn by Cajal based on his Golgi-stained material (Cajal, 1995). The use of two different rabbit antibodies against the subunit 1 of the NMDA receptor (D, R- 04/13; E, AB 1516; see Table 1) results in a very similar staining pattern (compare D and E). Immunoreactivities are most intense in the CA1 area, where the apical dendrites (running downwards in B) in the stratum radiatum (SR) are prominent (D, inset; E, inset), while the stratum oriens (SO; B) and the DG (C; ML - molecular layer, MF - mossy fibers) display less intensity. A similar pattern is observed after immunostaining with the monoclonals of "pattern group 1 patients" (representative examples: F, 007-168; H, 008-218) with anti- NMDA receptor encephalitis. In "pattern group 2" patients (representative examples: G, 003-102; I, G-16/04), the pattern is quite different, presenting as the same disorder based on laboratory and clinical criteria. Here the immunoreactivity in the stratum oriens of the CA1 region and the inner molecular layer of the DG are most prominent (G, I), while CA1 and DG cell bodies are negative. Bar indicates 600 µm in (D) to (I).

2.5. Targets of pattern group 1 and group 2 monoclonals or CSF samples display different ultrastructural localizations in the hippocampus of the rat

The striking differences in the light microscopic immunostaining patterns between pattern group 1 and pattern group 2 are due to distinct subcellular targets as demonstrated by electron microscopy. For optimal visualization, flat embedded cryostat sections were mounted upright on a perspex support. Subsequent semithin sections demonstrate the complete thickness of the cryostat tissue, disclosing immunostained synapses as black dots. This procedure provides an optimal orientation of synapses in adjacent ultrathin sections (Fig. 5A to C).

As expected, rabbit antibodies against the NR1 subunit of the NMDA receptor produce strong labeling of postsynaptic structures in the CA1 region of the rat hippocampus (Fig. 5A, asterisks), The group 1 CSF sample staining pattern is not as strong as above, but the postsynaptic

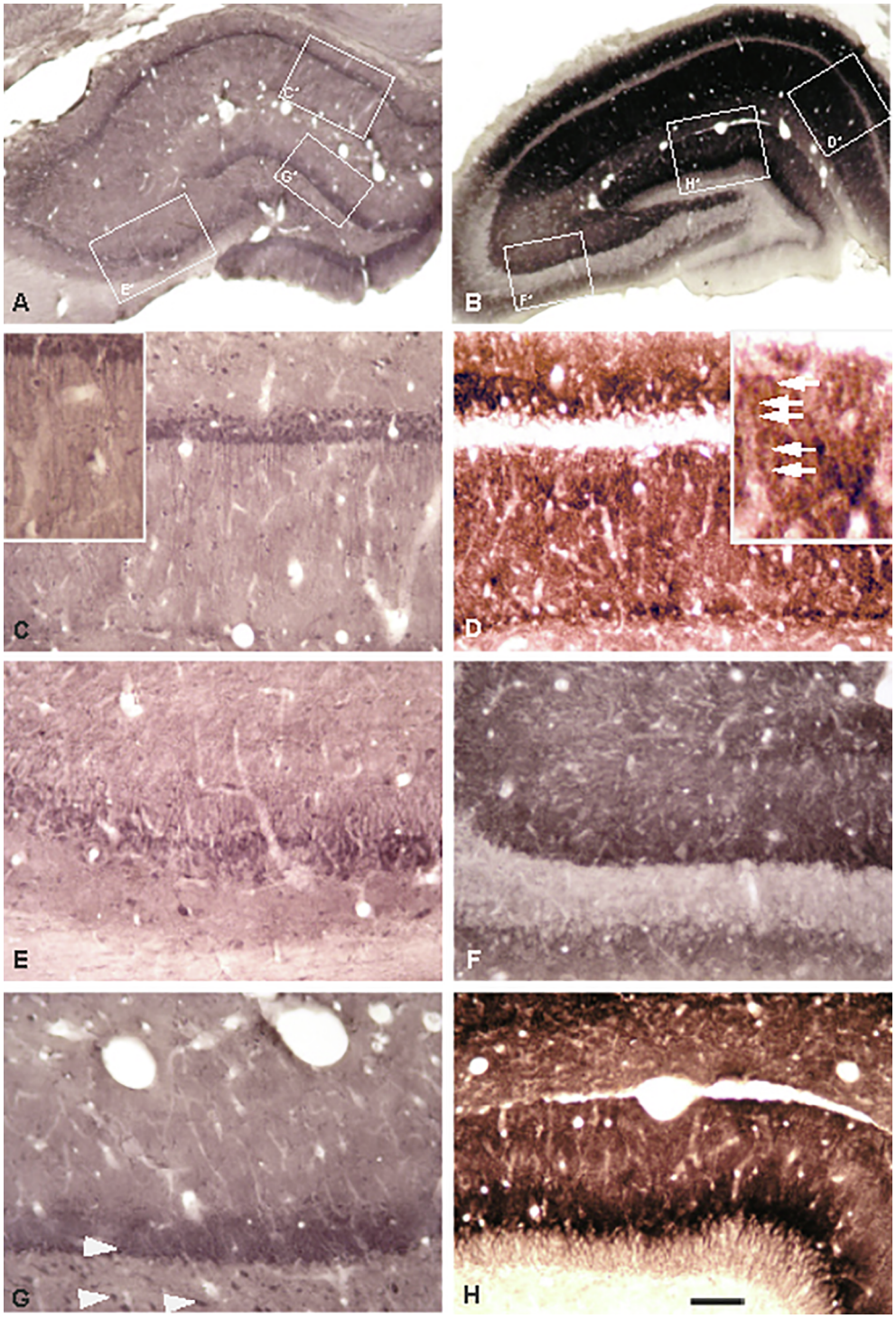

Fig. 3. Two groups of patients with NMDA-encephalitis display strikingly different hippocampal CSF-staining patterns especially at high magnification. Three hippocampal areas, the CA1 region, the CA3 region and the upper blade of the DA (surveys in A, B; areas boxed in A), are selected for detailed analysis at higher magnification. In the CA1 region, CSF samples and monoclonals of "group 1 patients" (see: 008-218) react with the cell bodies of pyramidal neurons and with the main dendrites throughout most of the stratum radiatum (B). This corresponds well with the distribution of NMDA-R1 receptor subunits as visualized with recognized rabbit antibodies (compare to Fig. 2D, E; insets). In contrast, CSF samples and a CSF-derived monoclonal antibody (G-16/04) from "group 2 patients" display pyramidal neurons with empty cell bodies (D). Note that even the main dendrites can be recognized as tubes between the strongly reactive neuropil (D, arrows in inset). In the CA3 region the situation is quite similar (E, F). In the DG pattern group 1 CSF samples (G) react with the cell bodies of granule cells as well as with those of interneurons below (G, arrows). Note that the DG granule cell layer is at the same level in (G) and (H). CSF samples and CSF-derived monoclonal antibody of "group 2 patients" do not react with granule cell bodies (H). Instead, strong immunoreactivity is found in the neuropil of the lower molecular layer (H). Bar in (H) indicates 300 μm in (A) and (B) and 100 μm in (C) to (H).

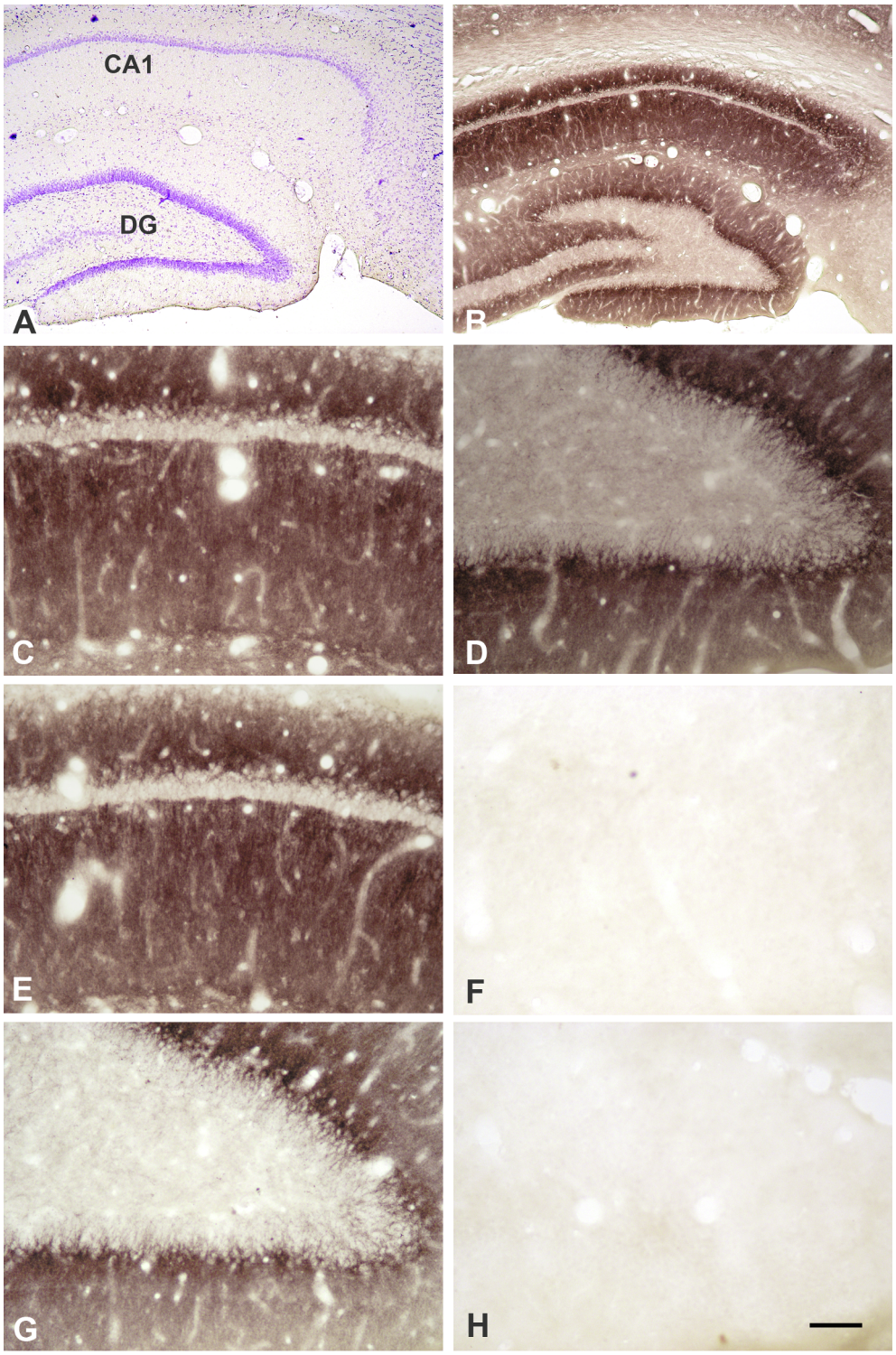

Fig. 4. CSFs and CSF-derived monoclonal antibodies of "pattern group 1 patients" do interact with the NMDA-R1 subunit of NMDA receptors. For gross orientation CA1 and DG subareas (stratum oriens, SO; stratum radiatum, SR; DG molecular layer, ML) are indicated in a coronal section across the hippocampus after staining with cresyl violet (A). Staining of an adjacent section with a CSF-derived monoclonal antibody of a group 2 patient (003 102) without any pretreatment (Table 3, experiment 1a) resulted in the typical group 2 staining pattern, with a dark SO, negative pyramidal and granule cell bodies and a strongly positive DG lower molecular layer (B, details in C and D; compare to Table 2). Preincubation of an adjacent section with a rabbit anti-NMDA-R1 antibody (Table 3, experiment 1b) does not alter the result (not shown). This fact indicates that the rabbit anti-NMDA-R1 antibody does not interact with the same epitope as the monoclonal does. Turning over the sequence and using the CSF-derived monoclonal antibody of a group 2 patient (003 102) first without pretreatment (Table 3, experiment 2a), the typical group 2 staining pattern is obtained (E, G). When, however, the adjacent section was pretreated with the rabbit anti-NMDA-R1 antibody before the pattern group 2 monoclonal (Table 3, experiment 2b), immunoreactivity with the anti-rabbit secondary antibody was abolished completely (F, H; see Table 3). This indicates that the CSF of the group 2 patients indeed interacts with the NMDA-R1 subunit, binding to an epitope which also is recognized by the rabbit antibody. Bar in (H) indicates 320 μm in (A) and (B) and 80 μm in (C) to (H).

localization of the immunoractivity (Fig. 5B, asterisk) is evident. In contrast, treatment with pattern group 2 monoclonals leads to reaction in the presynaptic compartment (Fig. 5C, asterisk), while the postsynaptic area, as identified by the dark postsynaptic density (Fig. 5C, arrow), remains empty.

3. Discussion

About one decade ago antibody-mediated neurological disorders were considered to be rare events. This concept was prominently revised when it was recognized that a number of patients, presenting with prominent neuropsychiatric symptoms like amnesia, seizures, frequent dyskinesias, autonomic dysfunction, and decreased level of consciousness, had serum/cerebrospinal fluid antibodies that reacted principally with the neuropil of hippocampus, apparently with the NMDA-R1 subunit of the NMDA receptor (Dalmau et al., 2007; Dalmau et al., 2008). A recent epidemiological study (Dubey et al., 2018) emphasized a threefold increase in the incidence of autoimmune encephalitides during the last ten years, most likely attributable to the increased identification of autoantibody-positive cases.

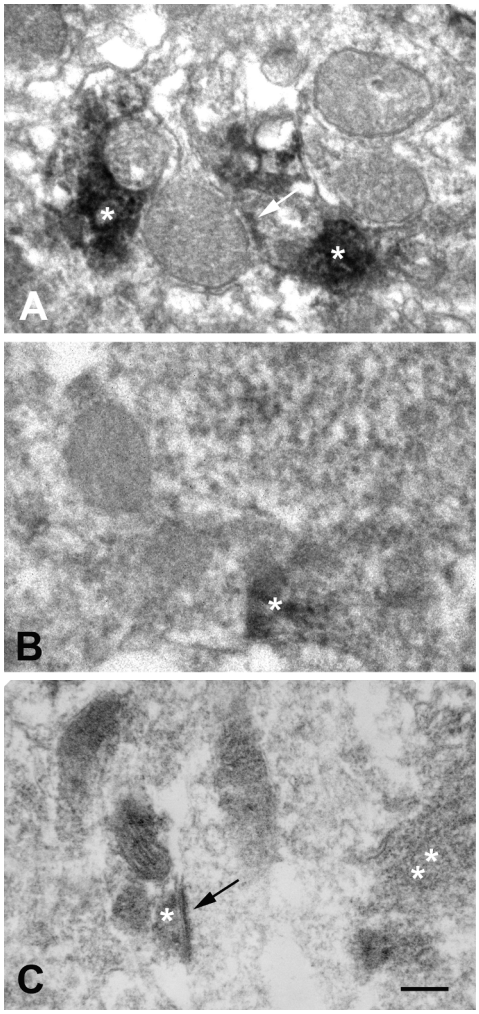

Fig. 5. Ultrastructural localization of the immunoreactivities obtained with "pattern group 1 or group 2" CSF samples and CSF-derived monoclonal antibodies. For primary detection of NMDA-R1 receptors, pattern group 1 or pattern group 2 immunoreactivites at the light microscopic level cryostat sections were flat embedded in araldite and mounted in upright position on a perspex support (see methods). Black dots representing immunopositive subcellular areas are localized on overmagnified semithin sections (not shown). Characteristic vessels or tissue defects were used to relocalize the positions of adjacent ultrathin sections. Synaptic NMDA-R1 receptor immunoreactivity as visualized with rabbit antibodies was always restricted to the postsynaptic area (A, asterisks) as identified by the postsynaptic density (A, white arrow). This was also the case in pattern group 1 CSF immunoreactivity (B asterisk). In contrast, pattern group 2 CSF immunoreactivity was localized presynaptically (C, white asterisks) and the postsynaptic area (C, black asterisk) identified by the prominent postsynaptic density (C, arrow) remained unstained. Bar in (C) indicates 400 nm in (A), (B), and (C).

However, the extraordinary diversity of symptoms in patients with recognized anti-NMDA-R1 encephalitis raises the question, whether all the neurological problems of these patients are due to the autoimmune response to the NR1 subunit, ore more precisely, against the same splice variant of the NMDA receptor. One group of patients with anti-NMDA-R encephalitis has CSF antibodies directed against a single define epitope of the NMDA-R1 subunit (Gleichman et al., 2012). However, other antibodies may be present in patients suffering from the disease (Kreye et al., 2016).

3.1. Technical considerations

Currently, anti-NMDA-R encephalitis is diagnosed using clinical criteria (Graus et al., 2016) together with the detection of anti-NMDA-R1 antibodies in CSF samples of these patients. Such antibodies may be detected by NMDA-R1-cDNA transfected HEK-cells or in uncertain cases with hippocampal sections of animals, mostly rodent brains. For this purpose, immunofluorescence procedures are typically used on cryostat sections mounted on glass slides after sectioning.

This procedure links two disadvantages. First, immunostaining of mounted sections is about 10-fold less sensitive when compared to the staining of freely floating sections (unpublished observations). Second, immunofluorescence per-se is not a very sensitive technique. This fact becomes most evident when comparing Fig. 1B and F. Using immunofluorescence for staining at 10-fold dilution of the CSF the cytoplasm of CA1 cell bodies is NMDA-R1-positive, but dendrites are not stained. In contrast, the same CSF at the same dilution, after the immunoperoxidase procedure (ABC-technique) demonstrates NMDA-R1-positive dendrites in addition to the cell bodies the (Fig. 1F). Furthermore, the immunoperoxidase procedure allows analysis of CSF-immunostained tissue sections at the electron microscopic level. This offers the possibility to confirm, whether immunoreactive deposits are found in pre- or postsynaptic localizations (see Fig. 5). Due to our efforts to support animal welfare, instead of perfusing additional rats, our brains had been cryoportected and frozen for quite a number of years. Unfortunately, this approach compromises to some degree the quality of electron microscopic images.

3.2. CSF-derived and monoclonal antibodies from patients in pattern group 2 patients do not correspond to the familiar localization of NMDA receptor 1 in the rat brain hippocampus

The staining pattern of the NMDA receptor in the rat hippocampus is typically characterized by CA1 neurons with a strongly positive cytoplasm (Table 1) standing out as bright line (immunofluerescence) or as dark line (immunoperoxidase visualization) already in survey micrographs (Fig. 2D, E). NMDA-R1-like immunoreactivity extends into the main dendrites, which may be discerned as descending threats throughout the stratum radiatum (Fig. 2D, E).

The most surprising difference between the staining patterns of CSFs from pattern group 1 and pattern group 2 patients is the fact that only pattern group 1 CSFs reproduce the familiar distribution of the NMDA receptor 1 in the hippocampus (Petralia et al., 1994; Johnson and Jiang, 1996). Even more surprising is the fact that almost all published figures, which supposedly demonstrate NMDA receptors (Dalmau et al., 2007, Fig. 3A; Dalmau et al., 2008, Fig. 1A; Peery et al., 2012, Fig. 1; Dalmau, 2016, Fig. 1A; Kreye et al., 2016, Fig. 1A, 2L; McCracken et al., 2017, Fig. 2d; Dalmau & Graus, 2018, Fig. 1c; Hara et al., 2018, Fig. 2G, H), do not correspond to the widely accepted localization of the NMDA-R1 protein in the rat hippocampus (Petralia et al., 1994; Johnson and Jiang, 1996; present report Fig. 2D, E). In all the cited figures cell bodies of the CA1 neurons remain unstained, featuring as dark line in immunofluorescence visualization Table 2.

3.3. The familiar pattern of NMDA-R1 localization in the rat hippocampus may be due to the C-terminal specificity of available antibodies

Attempts to understand the morphological localization of the NMDA-R1 in the mammalian brain depend largely on two approaches: (1) visualizing the mRNA message by in-situhybridization or/and (2) visualizing the protein product by immunocytochemistry. The differentiation between the NMDA-R1-a and NMDA-R1-b splice variants (absence or presence of the N-cassette; see Table 4) seems less significant important, when regarding the NMDA-R1 message (Laurie et al., 1995). In contrast, the combination of the preterminal and C-terminal sequences strongly affects the localization of the corresponding NMDA-R1 in the hippocampus. Apparently, NMDA-R1s with C2-type terminal sequences (see Table 4) are strongly expressed (see Fig. 4; Laurie et al., 1995), while those with C2′-type terminals are

absent (GluR3a/b) or expressed only weakly (GluR4a/b) in the CA1 region and the DG Table 3.

Immunocytochemical visualization of the NMDA-R1 is prone to failure, when available antibodies do not recognize all variants of the protein. The NMDA-R1 subunit of the NMDA receptor, however, is expressed in form of eight splice variants (Paoletti et al., 2013). There is one preterminal peptide (C1) and two distinct types of C-terminal peptides (C2 and C2′, see Table 4). Unfortunately, all available rabbit anti-NMDA-R1 antibodies (see Table 1) have been raised against C2-containing terminal peptides of the NMDA-R1 protein. No antibodies against C2-ending NMDA-R1s are available Table 4.

Consequently, the familiar pattern of the NMDA-R1 distribution in the hippocampus, which displays strongly stained somata and primary dendrites of CA1 and CA3 neurons (Petralia et al., 1994; Hollmann et al., 1993; this report Figs. 2 and 3) reflects the regional distribution of NMDA-R1 splice variants with the common core and C2-type terminals. The direct consequence of this conclusion is the fact that any antibody directed against the NMDA-R1 protein (excluding the N-casette and the C2′ terminal peptide) will produce the same staining pattern.

The converse conclusion indicates that antibodies such as the 003-102 monoclonal antibody or those contained in the G-16/04 CSF, which do not stain somata and principal dendrites of CA1 and CA3 neurons, are blocked from interaction by conformations, which shield C-terminal sequences, or must be specific for C2-containing splice variants. The latter idea appears likely when such variants such as the GluN1-3 or the GluN1-4 subtype are absent in the hippocampus. Accordingly, the negative staining pattern of CA1 and CA3 neurons is readily explained.

Indeed, the GluN1-3 splice variant is not expressed in the hippocampus (Laurie et al., 1995), while the Glu1-4 variant is present. In the latter case, unstained cell bodies may be explained if the GluN1-4 protein is produced in CA1 and CA3 neuronal somata, but effectively transported to axons or axon terminals, leaving the cell body. The existence of presynaptic NMDA-Rs has been controversial for decades, but is now generally accepted (Banerjee et al., 2016). This idea of a presynaptic localization of GluN1-4 type NMDA-R1s is further supported by the fact that our electron microscopical experiments disclose that only one single anti-NMDA-R1 antibody stains presynaptic terminals. This is the G-16/4 CSF, which apparently recognizes the C2-terminal splice variant. Additional investigations are needed to ascertain the potential presynaptic localization of the GluN1-4 splice variant of the NMDA-R1 subunit.

3.4. Conclusion

CSF-derived autoantibodies from patients with diagnosed anti-NMDA-autoimmune encephalitis, when analyzed with rat brain sections, show at least two distinct patterns of immunoreactivity. Antibodies from pattern group 1 patients display the familiar pattern of NMDA-R1 distribution in the hippocampus with strongly stained cell bodies and primary dendrites in the CA1 and CA3 region, in line with the predominant postsynaptic localization of the NMDA receptor in the brain. Autoantibodies from pattern group 2 patients, however, show an inverse pattern, leaving cell bodies and primary dendrites in CA1 and CA3 regions largely empty. The present data indicate that autoantibodies of pattern group 1 patients interact with postsynaptical NMDA receptors, while those of pattern group 2 patients preferentially target presynaptic NMDA receptors. Consequently, it will be very interesting to determine, whether pattern group 1 and 2 patients display distinct clinical phenotypes. Ongoing studies will answer this question.

4. Experimental procedure

4.1. Chemicals

Chemicals were obtained from Sigma-Aldrich GmbH, Taufkirchen, Germany, if not indicated otherwise. Sources of primary antibodies are described below. Biotin labeled secondary antibodies and the Elite ABC complex were from Vector (Vector Laboratories, Burlingame, CA, USA).

4.2. Study approval

All animal experiments were approved by the Regional Berlin Animals Ethics Committee and conducted in strict accordance with the European Communities Council directive regarding care and use of animals for experimental procedures. Adult male Wistar rats, weighing 250–300 g were obtained from our institutional breeder (Department for Experimental Medicine (FEM), Charité University Medicine Berlin).

Table 1
Types and Sources of Antibodies.

Code/CatNr	Group	Host	Type	Conjugate	Antigen	Epitope	Provider
AB 1516 (*)	1	rabbit	polyclonal	–	GluNR1	C-terminal C2	Chemicon 2007
R-04/13	1	rabbit	polyclonal	–	GluNR1	C-terminal C2	Gregor Laube
not available	?	rabbit	polyclonal	–	GluNR1	C-terminal C2	none
003–102	2	human	monoclonal	–	GluNR1	contains N368	Harald Prüss
008–218	1	human	monoclonal	–	GluNR1	contains N368	Harald Prüss
007–168	1	human	monoclonal	–	GluNR1	contains N368	Harald Prüss
G-15/05	2	human	CSF	–	GluNR1	unknown	Harald Prüss
G-15/11	1	human	CSF	–	GluNR1	unknown	Neurology Jena
G-16/04	2	human	CSF	–	GluNR1	unknown	Harald Prüss
J-18/40	1	human	CSF	–	unknown	unknown	Neurol. Oberhausen
BA-3000	–	goat	polyclonal	biotin	human IgG	–	Vector laboratorial
BA-1000	–	goat	polyclonal	biotin	rabbit IgG	–	Vector laboratories
A-11008	–	goat	polyclonal	alexa 488	rabbit IgG	–	Invitrogen
A-11013	–	goat	polyclonal	alexa 488	human IgG	–	Invitrogen

(*) The AB 1516 antibody from Chemicon was excellent, but is no longer available. Unfortunately Chemicon, which belongs to Merck-Millipore, have replaced the previous sample by a rabbit monoclonal antibody (AB 9864). This antibody was ineffectual (it worked only very weakly in our hands) and Merck-Millipore was not prepared to refund our costs.

Table 2
Autoantibodies in the CSFs of group 1 or group 2 patients yield different immunostaining patterns in the rat hippocampus.

	group 1	group 2
CA1 region		
stratum oriens (SO)	weak	strong
pyramidal cells	strong	negative
pyramidal main dendrites	strong	negative
dentate gyrus (DG)		
lower molecular layer	negative	strong
granula cell layer	strong	negative

Table 3
Blocking experiments. For blocking experiments freely floating cryostat sections first were incubated for 24 h in the selected primary antibody (AB) to potentially block its epitope. After washing the sections were then incubated with the second primary AB and the subsequent detection reagents. If the epitope of the second primary AB is the same as that of the first primary AB, which is blocked in this case, no signal is obtained (experiment 2b).

First primary AB	Second primary AB	2. antibody	Signal system	Result
experiment 1a				
–	003–102	anti-human IgG	ABC	+ + +
experiment 1b				
R-04/13	003–102	anti-human IgG	ABC	+ + +
experiment 2a				
–	R-04/13	anti-rabbit IgG	ABC	+ + +
experiment 2b				
003–102	R-04/13	anti-rabbit IgG	ABC	Ø

Animals were housed in group-cages under controlled temperature (22 °C) and illumination (12 h cycle) with water and food ad libitum. All clinical investigations were conducted according to Declaration of Helsinki principles. Written informed consent was received from participants at the Charité or the university Jena, Departments of Neurology, or their representatives prior to inclusion in the study and analyses were approved by the Charité University Hospital Institutional Review Board.

4.3. Brain tissue blocks

Rats were deeply anaesthetized and fixed via transcardial perfusion with a solution consisting of 4% paraformaldehyde, 0.05% glutaraldehyde, and 0.2% picric acid in 0.1 M phosphate buffer, pH 7.4 (Somogyi and Takagi, 1982). Brains were removed, cryoprotected in 0.4 M sucrose for about 4 h and in 0.8 M sucrose overnight, cut into blocks at preselected rostrocaudal levels, shock-frozen in hexane at −70 °C, and stored at −80 °C until use as described previously (Wagner et al., 2016).

4.4. Antibodies and cerebrospinal fluids

Two different rabbit anti-NMDA-R1 receptor antibodies were used. The reference antibody, raised against the synthetic C-terminal peptide (LQNQKDTVLPRRAIEREEGQLQLCSRHRES), was used for the original localization of the NMDA-R1 (Petralia et al., 1994). This antibody was commercially obtained from Chemicon (AB1516; for details see Table 1) and is known to recognize four of the eight splice variants of the NMDA-R1 protein (Petralia et al., 1994). A second anti-NMDA-R1 antibody was raised in our laboratory (Laube et al., unpublished) against the same C-terminal peptide. Cerebrospinal fluid samples of six patients with anti-NMDA-R encephalitis (G-15/05, G- 15/11, G-16/04, G-16/11, J-18/40; see Table 1) and three human monoclonal anti-NMDAR1 antibodies from three patients (003-102, 007-168, 008-218, see Table 1) were selected as representative samples. Monoclonal antibodies were generated by cloning of full-length immunoglobulin G variable heavy and light chain genes from single antibody-secreting cells. All human CSF-samples and antibodies showed the characteristic binding to NMDA-R1- expressing human embryonic kidney (HEK293) cells and to murine brain sections (Kreye et al., 2016; Ly et al., 2018).

4.5. Immunocytochemistry

For immunofluorescence analysis, cryostat sections were mounted on gelatin-coated slides and pretreated with the permeabilizing solution (see next paragraph). Sections on slides were incubated overnight with primary antibody or CSF, washed in PBS, and pretreated with PBSA (0.2% bovine serum albumin in PBS). After 2 h treatment with a fluorescently labeled secondary antibody (1:1000) section were washed, coverslipped with fluoromount, and analysed in a fluorescence microscope. For immunoperoxidase immunocytochemistry, freely floating coronal brain cryostat sections (25 mm) were subjected to immunocytochemistry as described earlier (Wagner et al., 2016). In short, sections were rinsed in phosphate buffered saline (PBS) and treated for 15 min with 1% sodium borohydride in PBS to remove residual aldehyde groups from the fixative. Sections were pretreated for 30 min in a blocking and permeabilizing solution (10% normal goat serum in 0.3% Triton X-100 and 0.05% phenylhydrazine in PBS at room temperature (RT). Anti-NMDA-R1 antibodies and CSFs (Table 1) were applied for 36 h at appropriate dilutions in PBS containing 10% NGS, 0.3% Triton X-100, 0.1% sodium azide, and 0.01% thimerosal at 4° C. Sections were thoroughly rinsed in PBS, pretreated for 1 h with PBS-A, and exposed for another 24 h at RT to the secondary antibody, diluted 1:5,000 in PBS-A containing 0.1% Triton X- 100. After repeated washings in PBS and preincubation for one hour in PBS-A, the Elite avidin–biotin-peroxidase-complex (1:200 dilution in PBS-A) was attached to biotinylated secondary antibodies for another 12 h at RT. After additional rinses in PBS, preincubation for 15 min in a solution of 0.5 mg/ml diaminobenzidine, 3 mg/ml ammonium nickel sulfate, and 10 mM imidazole in 50 mM Tris buffer, pH 7.6, the visualization of the antigen–antibody complexes was started by the addition of 0.0015% hydrogen peroxide and stopped after 15 min at RT by repeated washings with PBS. Sections were mounted onto gelatine-coated slides, air-dried not longer than 30 min, dehydrated through a graded series of ethanol, transferred into xylene, and coverslipped with entellan.

4.6. Immunocytochemistry with electron microscopic analysis

Immunocytochemistry with freely floating sections was performed as described above with the exception that only the preincubation step before the primary antibody solutions contained 0.1% Triton X-100. After visualization of the antigen–antibody-ABC complexes with DAB/nickel and hydrogen peroxide as described above, sections were post-fixed in 1% osmium tetroxide for 30 min, dehydrated, and flat embedded in araldite. Semithin sections and interposed ultrathin sections were cut with a Leica Ultracut microtome. Semithin sections were stained with 1% toluidine blue, pH 9.3, and photographed with a Leica DMRB photomicroscope. Ultrathin sections were contrasted with uranyl acetate followed by lead citrate (Reynolds, 1963) and examined using a Zeiss EM900 electron microscope.

4.7. Nissl stain

Sections are mounted from PBS on gelatin-coated glass slides and dried for 30 min at RT. Subsequently they were left in 70% ethanol overnight, rinsed in bidistilled water, and stained with cresyl violet (0.2% cresyl violet acetate in 20 mM acetate buffer, pH 4.0) for 30 min at RT (Geisler et al., 2002). After rinsing in bidistilled water, sections were dehydrated fast through a graded series of ethanol, transferred into xylene, and coverslipped with Entellan.

Table 4
Important domains of the NMDA receptor NR1 subunit. C-terminals are given for NMDAR1-1 and NMDAR1-2 as C2 and for NMDAR1-3 and NMDAR1-4 as C2′.

Nomenclature	Nomenclature	Nomenclature	N-casette	pre-C-terminal (C1)	C-terminal (C2 or C2′)
Hollmann et al., 1993	Paoletti et al., 2013	Laurie et al., 1995			
NMDAR1-1a	GluN1-1a	NR1-1	missing	DRKSGR AEPDPKKKAT FRAITSTLAS SFKRRRSSKDT	STGGGR GALQNQKDTVL PRRAIEREEG QLQLCSRHRES
NMDAR1-1b	GluN1-1b	NR1-1	QYHPTDITGPLN LSDPSVSTVV	DRKSGR AEPDPKKKAT FRAITSTLAS SFKRRRSSKDT	STGGGR GALQNQKDTVL PRRAIEREEG QLQLCSRHRES
NMDAR1-2a	GluN1-2a	NR1-2	missing	missing	STGGGR GALQNQKDTVL PRRAIEREEG QLQLCSRHRES
NMDAR1-2b	GluN1-2b	NR1-2	QYHPTDITGPLN LSDPSVSTVV	missing	STGGGR GALQNQKDTVL PRRAIEREEG QLQLCSRHRES
NMDAR1-3a	GluN1-3a	NR1-3	missing	DRKSGR AEPDPKKKAT FRAITSTLAS SFKRRRSSKDT	QYHPTDIT GPLNLSDPS VSTVV
NMDAR1-3b	GluN1-3b	NR1-3	QYHPTDITGPLN LSDPSVSTVV	DRKSGR AEPDPKKKAT FRAITSTLAS SFKRRRSSKDT	QYHPTDIT GPLNLSDPS VSTVV
NMDAR1-4a	GluN1-4a	NR1-4	missing	missing	QYHPTDIT GPLNLSDPS VSTVV
NMDAR1-4b	GluN1-4b	NR1-4	QYHPTDITGPLN LSDPSVSTVV	missing	QYHPTDIT GPLNLSDPS VSTVV

Declarations

Ethics approval and consent to participate.

All animal experiments were approved by the Regional Berlin Animals Ethics Committee and conducted in strict accordance with the European Communities Council directive regarding care and use of animals for experimental procedures. Adult male Wistar rats, weighing 250- 300 g were obtained from our institutional breeder (Department for Experimental Medicine (FEM), Charité University Medicine Berlin). Animals were housed in group-cages under controlled temperature (22° C) and illumination (12 hour cycle) with water and food ad libitum. All clinical investigations were conducted according to Declaration of Helsinki principles. Written informed consent was received from participants at the Charité or the university Jena, Departments of Neurology, or their representatives prior to inclusion in the study and analyses were approved by the Charité University Hospital Institutional Review Board.

Consent for publication

Not applicable.

Availability of data and materials

The data sets used and/or analysed during the current study are available from the corresponding author on reasonable request.

Funding

IZKF Jena provided a scholarship as clinical scientist to F.W.

Authors contributions

FW and RWV performed the experiments, analyzed and interpreted the data and were major contributors in writing the manuscript. AG and OK performed experiments and contributed in writing the manuscript. GL developed the R-04/13 antibody. JK, HP provided human CSFs and characterized the monoclonal antibodies and contributed critical aspects for discussion. OWW contributed in writing the manuscript and provided important aspects for discussion. All authors read and approved the final manuscript.

Declaration of Competing Interest

The authors declare that they have no known competing financial interests or personal relationships that could have appeared to influence the work reported in this paper.

Acknowledgements

The authors gratefully acknowledge the invaluable help of Dr. Agnieszka Münster-Wandowski in maintaining the electron microscope in optimal working condition and for continuous technical and scientific support. Special thanks are due to Prof. Dr. A. P. Corfield for critically reading the manuscript.

References

Banerjee, A., Larsen, R.S., Philpot, B.D., Paulsen, O., 2016. Roles of presynaptic NMDA receptors in neurotransmission and plasticity. Trends Neurosci. 39 (1), 26–39. https://doi.org/10.1016/j.tins.2015.11.001.

Cajal, R.S., 1995. Histology of the Nervous System of Man and Vertebrates. Oxford University Press, Oxford.

Dalmau, J., 2016. NMDA receptor encephalitis and other antibody-mediated disorders of the synapse: The 2016 Cotzias Lecture. Neurology. 87 (23), 2471–2482. https://doi.org/10.1212/WNL.0000000000003414.

Dalmau, J., Gleichman, A.J., Hughes, E.G., Rossi, J.E., Peng, X., Lai, M., Dessain, S.K., Rosenfeld, M.R., Balice-Gordon, R., Lynch, D.R., 2008. Anti-NMDA-receptor encephalitis: case series and analysis of the effects of antibodies. Lancet Neurol. 7, 1091–1098. https://doi.org/10.1016/S1474-4422(08)70224-2.

Dalmau, J., Graus, F., 2018. Antibody-mediated encephalitis. N Engl. J. Med. 378 (9), 840–851. https://doi.org/10.1056/NEJMra1708712.

Dalmau, J., Tüzün, E., Wu, H.Y., Masjuan, J., Rossi, J.E., Voloschin, A., Baehring, J.M., Shimazaki, H., Koide, R., King, D., Mason, W., Sansing, L.H., Dichter, M.A., Rosenfeld, M.R., Lynch, D.R., 2007. Paraneoplastic anti-N-methyl-D-aspartate receptor encephalitis associated with ovarian teratoma. Ann Neurol. 61:25-36. doi:10.1002/ana.21050.

de Witte, L.D., Hoffmann, C., van Mierlo, H.C., Titulaer ,M.J., Kahn, R.S., Martinez-Martinez, P., 2015. Absence of N-Methyl-D-Aspartate Receptor IgG Autoantibodies in Schizophrenia: The Importance of Cross-Validation Studies. JAMA Psychiatry. 72:731- 3. doi: 10.1001/jamapsychiatry.2015.0526.

Dubey, D., Pittock, S.J., Kelly, C.R., McKeon, A., Lopez-Chiriboga, A.S., Lennon, V.A., Gadoth, A., Smith, C.Y., Bryant, S.C., Klein, C.J., Aksamit, A.J., Toledano, M., Boeve, B.F., Tillema, J.M., Flanagan, E.P., 2018. Autoimmune encephalitis epidemiology and a comparison to infectious encephalitis. Ann. Neurol. 83 (1), 166–177. https://doi.org/10.1002/ana.25131.

Geisler, S., Heilmann, H., Veh, R.W., 2002. An optimized method for simultaneous demonstration of neurons and myelinated fiber tracts for delineation of individual trunco- and palliothalamic nuclei in the mammalian brain. Histochem. Cell Biol. 117 (1), 69–79. https://doi.org/10.1007/s00418-001-0357-z.

Gleichman, A.J., Spruce, L.A., Dalmau, J., Seeholzer, S.H., Lynch, D.R., 2012. Anti-NMDA receptor encephalitis antibody binding is dependent on amino acid identity of a small region within the GluN1 amino terminal domain. J. Neurosci. 32 (32), 11082–11094. https://doi.org/10.1523/JNEUROSCI.0064-12.2012.

Görtzen, A., Schlüter, S., Veh, R.W., 2004. Anti-astrocyte Autoantibodies in Guillain–Barré Syndrome – Possible involvement in the pathophysiology of a psychosyndrome? Autoimmunity. 37, 521–528. https://doi.org/10.1080/08916930412331279840.

Graus, F., Titulaer, M.J., Balu, R., Benseler, S., Bien, C.G., Cellucci, T., Cortese, I., Dale, R.C., Gelfand, J.M., Geschwind, M., Glaser, C.A., Honnorat, J., Höftberger, R., Iizuka, T., Irani, S.R., Lancaster, E., Leypoldt, F., Prüss, H., Rae-Grant, A., Reindl, M., Rosenfeld, M.R., Rostásy, K., Saiz, A., Venkatesan, A., Vincent, A., Wandinger, K.P., Waters, P., Dalmau, J., 2016. A clinical approach to diagnosis of autoimmune encephalitis. Lancet Neurol. 15 (4), 391–404. https://doi.org/10.1016/S1474-4422(15)00401-9.

Hara, M., Martinez-Hernandez, E., Ariño, H., Armangué, T., Spatola, M., Petit-Pedrol, M., Saiz, A., Rosenfeld, M.R., Graus, F., Dalmau, J., 2018. Clinical and pathogenic significance of IgG, IgA, and IgM antibodies against the NMDA receptor. Neurology. 17 (90), e1386–e1394. https://doi.org/10.1212/WNL.0000000000005329.

Hsu, S.M., Soban, E., 1982. Color modification of diaminobenzidine (DAB) precipitation by metallic ions and its application for double immunohistochemistry. J. Histochem. Cytochem. 30, 1079–1082. https://doi.org/10.1177/30.10.6182185.

Hollmann, M., Boulter, J., Maron, C., Beasley, L., Sullivan, J., Pecht, G., Heinemann, S., 1993. Zinc potentiates agonist-induced currents at certain splice variants of the NMDA receptor. Neuron. 10 (5), 943–954. https://doi.org/10.1016/0896-6273(93)90209-a.

Johnson, R.R., Jiang, X., 1996. Burkhalter A. Regional and laminar differences in synaptic localization of NMDA receptor subunit NR1 splice variants in rat visual cortex and hippocampus. J Comp Neurol. 6;368(3):335-55. doi: 10.1002/(SICI)1096-9861(19960506)368:3 < 335::AID-CNE2 > 3.0.CO;2-6.

Kreye, J., Wenke, N.K., Chayka, M., Leubner, J., Murugan, R., Maier, N., Jurek, B., Ly, L.T., Brandl, D., Rost, B.R., Stumpf, A., Schulz, P., Radbruch, H., Hauser, A.E., Pache, F., Meisel, A., Harms, L., Paul, F., Dirnagl, U., Garner, C., Schmitz, D., Wardemann, H., Prüss, H., 2016. Human cerebrospinal fluid monoclonal N-methyl-D-aspartate receptor autoantibodies are sufficient for encephalitis pathogenesis. Brain. 139, 2641–2652. https://doi.org/10.1093/brain/aww208.

Lalo, U., Pankratov, Y., Kirchhoff, F., North, A., Verkhratsky, A., 2006. NMDA receptors mediate neuron-to-glia signaling in mouse cortical astrocytes. J. Neurosci. 26, 2673–2683. https://doi.org/10.1523/jneurosci.4689-05.2006.

Laurie, D.J., Putzke, J., Zieglgänsberger, W., Seeburg, P.H., Tölle, T.R., 1995. The distribution of splice variants of the NMDAR1 subunit mRNA in adult rat brain. Brain Res. Mol. Brain Res. 32 (1), 94–108. https://doi.org/10.1016/0169-328X(95)00067-3.

Ly, L.T., Kreye, J., Jurek, B., Leubner, J., Scheibe, F., Lemcke, J., Wenke, N.K., Reincke, S.M., Prüss, H., 2018. Affinities of human NMDA receptor autoantibodies: implications for disease mechanisms and clinical diagnostics. J. Neurol. 265 (11), 2625–2632. https://doi.org/10.1007/s00415-018-9042-1.

McCracken, L., Zhang, J., Greene, M., Crivaro, A., Gonzalez, J., Kamoun, M., Lancaster, E., 2017. Improving the antibody-based evaluation of autoimmune encephalitis. Neurol. Neuroimmunol. Neuroinflamm. 4 (6). https://doi.org/10.1212/NXI.0000000000000404.

Panzer, J., Lynch, D., 2013. Treatment of anti-NMDA receptor encephalitis—time to be bold? Nat Rev Neurol. 9, 187–189. https://doi.org/10.1038/nrneurol.2013.31.

Paoletti, P., Bellone, C., Zhou, Q., 2013. NMDA receptor subunit diversity: impact on receptor properties, synaptic plasticity and disease. Nat Rev Neurosci. 14 (6), 383–400. https://doi.org/10.1038/nrn3504.

Paxinos, G., Kus, L., Ashwell, K.W.S., Watson, C., 1999. Chemoarchitectonic Atlas of The Rat Forebrain. Academic Press, San Diego.

Paxinos, G., Watson, C., 1998. The Rat Brain in Stereotaxic Coordinates. Acabdemic Press LTd, SanDiegeo.

Peery, H.E., Day, G.S., Dunn, S., Fritzler, M.J., Prüss, H., De Souza, C., Doja, A., Mossman, K., Resch, L., Xia, C., Sakic, B., Belbeck, L., Foster, W.G., 2012. Anti- NMDA receptor encephalitis. The disorder, the diagnosis and the immunobiology. Autoimm Rev. 11 (12), 863–872. https://doi.org/10.1016/j.autrev.2012.03.001.

Petralia, R.S., Yokotani, N., Wenthold, R.J., 1994. Light and electron microscope distribution of the NMDA receptor subunit NMDAR1 in the rat nervous system using a selective anti-peptide antibody. J. Neurosci. 14, 667–696. https://doi.org/10.1523/JNEUROSCI.14- 02-00667, 1994.

Reynolds, E.S., 1963. The use of lead citrate at high pH as an electron-opaque stain in electron microscopy. J. Cell Biol. 17, 208–212. https://doi.org/10.1083/jcb.17.1.208.

Rink, C., Görtzen, A., Veh, R.W., Prüss, H., 2017. Serum antibodies targeting neurons of the monoaminergic systems in Guillain-Barré syndrome. J. Neurol. Sci. 15, 318–323. https://doi.org/10.1016/j.jns.2016.11.078.

Somogyi, P., Takagi, H., 1982. A note on the use of picric acid-paraformaldehydeglutaraldehyde fixative for correlated light and electron microscopic immunocytochemistry. Neurosci. 7, 1779–1783. https://doi.org/10.1016/0306-4522(82)90035-5.

Titulaer, M.J., McCracken, L., Gabilondo, I., Armangué, T., Glaser, C., Iizuka, T., Honig, L.S., Benseler, S.M., Kawachi, I., Martinez-Hernandez, E., Aguilar, E., Gresa-Arribas, N., Ryan-Florance, N., Torrents, A., Saiz, A., Rosenfeld, M.R., Balice-Gordon, R., Graus, F., Dalmau, J., 2013. Treatment and prognostic factors for long-term outcome in patients with anti-N-Methyl-D-Aspartate (NMDA) receptor encephalitis: a cohort study. Lancet Neurol. 12, 157–165. https://doi.org/10.1016/S1474-4422(12)70310-1.

van Coevorden-Hameete, M.H., Titulaer, M.J., Schreurs, M.W., de Graaff, E., Sillevis Smitt, P.A., Hoogenraad, C.C., 2016. Detection and characterization of autoantibodies to neuronal cell-surface antigens in the central nervous system. Front. Mol. Neurosci. 31, 37. https://doi.org/10.3389/fnmol.2016.00037.

Wagner, F., Bernard, R., Derst, C., French, L., Veh, R.W., 2016. Microarray analysis of transcripts with elevated expressionsin the rat medial or lateral habenula suggest fast GABAergic excitation in the medial habenula and habenular involvement in the regulation of feeding and energy balance. Brain Struct. Funct. 221 (9), 4663–4689. https://doi.org/10.1007/s00429-016-1195-z.